

Contents list available at CBIORE journal website

International Journal of Renewable Energy Development

Journal homepage: https://ijred.cbiore.id



Research Article

One pot microwave-assisted synthesis of 2,5-dimethylfuran from bamboo hydrolysate in presence of green solvent and low-cost metal catalyst

Huei Yeong Lim a,b, Nor Adilla Rashidi a*o, Suzana Yusupco

Abstract. This study looked at the one-pot synthesis of 2,5-dimethylfuran (DMF) from glucose-rich bamboo hydrolysate using microwave heating technology in presence of green solvent, Low Transition Temperature Mixture (LTTM), and activated carbon-supported copper catalyst (Cu/AC). While DMF is mainly synthesized by using commercial glucose, the biomass with high cellulose content can also be used. Besides, the conventional synthesis that commonly employs organic solvents and noble metal catalysts has great toxicological and financial barriers. Thus, alternative cheaper and greener solvents and catalysts are needed, such as LTTM and carbon-supported copper. The bamboo hydrolysate was produced via acid hydrolysis with 0.5M sulphuric acid (H_2SO_4). LTTM was synthesized using choline chloride (ChCl) and malic acid, which were proven to be effective in DMF production in presence of H_2SO_4 . Reaction time, catalyst loading, and LTTM ratio were studied via response surface methodology with DMF yield as the response. Temperature was set at 120 °C in accordance with previous study. The LTTM was found to experience minimal mass loss at this reaction temperature. The Cu/AC catalyst was found to carry mostly reduced copper oxide (CuO) particles, with slight CuO residues, indicating successful synthesis of the catalyst. A quadratic regression model has been developed with R^2 =0.9481, with expected optimal condition at 1 min reaction time, 1% catalyst loading, and 4:1 LTTM ratio, with expected DMF yield of 25.61 mol% (13.67 mass percent). Experimental validation yielded 21.28 \pm 0.77 mol% (11.36 mass percent), indicating that this regression model was accurate. Overall, this study shown that the LTTM and Cu/AC are capable of producing DMF from biomass in one-pot manner.

Keywords: 2,5-dimethylfuran; activated carbon; biomass; copper catalyst; low transition temperature mixture.



@ The author(s). Published by CBIORE. This is an open access article under the CC BY-SA license (http://creativecommons.org/licenses/by-sa/4.0/).

Received: 15th January 2025; Revised: 19th March 2025; Accepted: 7th April 2025; Available online: 16th April 2025

1. Introduction

The global energy consumption is anticipated to continuously increase, and unfortunately in current state, fossil fuels remain as the main energy supply. Oil, coal, and natural gas are still the leading energy supplies, with shares of 30%, 27%, and 23%, respectively, in the year of 2023 (IEA, 2024). Among the renewables, bioenergy comprised of the largest chunk with more than half of the total renewable supply, outperformed the solar, wind, and hydro. However, this may not last long as the International Energy Agency (IEA) expected a significantly higher compounded average annual growth rate (CAAGR) on solar and wind of 19% and 12%, respectively, with no changes in stated policies globally (IEA, 2024). In comparison, CAAGR for bioenergy are just 2.9-7.7%. Despite that, bioenergy such as biomass-derived biofuels have multiple advantages over the solar and wind, whereby the biomass are notably versatile to produce various products according to the applications, and are commonly seen as carbon neutral (Seo et al., 2022). The carbon neutrality comes from the fact that the carbon dioxide (CO2)

emitted by the combustion of biomass or biofuels is equivalent to the CO_2 absorbed by these organisms during photosynthesis (Yadav et al., 2020). However, such traditional use of biomass via direct combustion, albeit being a carbon neutral energy source, possess health risk especially those coming from smoke and particulates released (Chakraborty & Mondal, 2018). Thus, converting the biomass to various "modern" biofuels and/or bioproducts are essential in ensuring the sustainability of the bioenergy industry.

Production of converted bioproducts can be performed, usually, via two main pathways: thermochemical and biological. Thermochemical methods involve the uses of heat energy to drive the chemical reactions, including torrefaction, pyrolysis, gasification, etc. (Jha et al., 2022; Lim, Rashidi, Othman, et al., 2023). On the other hand, biological technologies utilise microorganisms and other biological substrates to produce bioproducts, for example, anaerobic digestion and fermentation (Deivayanai et al., 2022). In this regard, the synthesis of 2,5-dimethylfuran (DMF) from biomass in thermochemical manners

^aChemical Engineering Department, Higher Institution Centre of Excellence - Centre for Biofuel and Biochemical Research, Institute of Sustainable Energy & Resources, Universiti Teknologi PETRONAS, Bandar Seri Iskandar, Malaysia

^bCentre for Carbon Capture, Utilisation, and Storage, Institute of Sustainable Energy & Resources, Universiti Teknologi PETRONAS, Bandar Seri Iskandar, Malaysia

^cGeneration Unit, Fuel and Combustion Section, TNB Research Sdn. Bhd., Kajang, Malaysia

^{*} Corresponding author
Email: adilla.rashidi@utp.edu.mv (N.A. Rashidi)

have great promise in the collective decarbonisation of energy supply. DMF is found to be a great biofuel as it s, among many, high in RON (119), energy density (about 30 MJ/L), and great fits with current conventional fuels used in internal combustion engines (Hoang et al., 2021). The production of DMF was discovered by Román-Leshkov et al. (2007) via the subsequent dehydration and hydrogenolysis of fructose into DMF, with 5-hydroxymethylfurfural (HMF) as the intermediate. Nowadays, other monosaccharides such as glucose with greater abundancy than fructose (Agarwal et al., 2018) can be utilised to synthesize HMF in acidic conditions (Endot et al., 2021). This significantly increased the potential HMF and DMF production capacities as compared to a decade ago through the utilization of high purity glucose.

Although the industrial production of glucose comes from the hydrolysis of starches, often from edible sources (Cereda, 2024), presence of carbohydrates and cellulose are also found in lignocellulosic biomass (Lim, Rashidi, Othman, et al., 2023; Wang et al., 2017). Besides, the abundance of lignocellulosic biomass, mainly comprised of agricultural and forestry residues, brings a huge advantage as the utilization of the biomass may divert a major portion of fossil fuels' dependency (Son Le et al., 2022). Despite that, biomass utilisation in the DMF production faces various challenges, particularly related to the recalcitrancy of lignocellulosic biomass in resisting the access of cellulose within its structure (Wang et al., 2019). Therefore, pretreatments such as acid hydrolysis are essential to extract the cellulose and convert into glucose beforehand. Nonetheless, separation and refining of the sugars from the biomass hydrolysate for the DMF production is not financially viable, costing around 30% of the capital cost (Morales et al., 2017). Moreover, as aforementioned, synthesis of intermediate HMF is favoured in acidic conditions, therefore this presented a possibility of direct utilisation of acidic hydrolysate coming from acid hydrolysis of biomass toward a sustainable and viable production of DMF.

In our previous study, it has been established that one-pot production of the intermediate HMF is possible by microwave-assisted heating and in presence of low transition temperature mixture (LTTM) (Lim, Rashidi, Cheah, & Abdul Manaf, 2023). Indeed, microwave-assisted heating is beneficial due to its great speed and efficiency (Gomes & Pastre, 2020), requiring only a few minutes instead of a few hours in a conventional batch reactor as demonstrated by Insyani et al. (2017). The DMF yield is also found to be slightly better with microwave irradiation than conventional heating (e.g., oil bath) (De et al., 2012).

With that, this study aims to expand and explore the direct synthesis of DMF in a similar one-pot manner from the liquid hydrolysate produced from acid hydrolysis of bamboo. In this case, the missing puzzle piece would be the suitable catalyst for the hydrogenolysis of HMF to DMF. Román-Leshkov et al. (2007) used a bimetallic catalyst consisted of ruthenium and copper, supported on commercial carbon in groundbreaking study. Since then, various noble and non-noble metals have been employed in the hydrogenolysis of HMF into DMF. He et al. (2024) presented a comprehensive review on the catalysts used in the past studies, whereby noble metals such as ruthenium, platinum, and palladium have reached a DMF yield of up to >99%, while non-noble metals including nickel, cobalt, and copper have produced over 90% of DMF yields. Here, copper is chosen as the low-cost metal in this study, which is supported on the commercial activated carbon and used in-situ in the microwave-assisted synthesis of DMF. Specifically, a three-factors five-levels response surface methodology is employed in performing the parametric study and optimization

of the direct DMF production by using the Central Composite Rotatable Design (CCRD).

2. Materials and Method

2.1 Materials

The raw bamboo (locally known as *buluh minyak* in Malay) is sourced within the vicinity of Tronoh, Perak, Malaysia. Concentrated analytical grade $98\%~H_2SO_4$ was procured from Fisher Chemical, which were diluted to various concentrations using deionized water for further experimental runs and uses. Reagent grade malic acid (>99.5%) and ChCl (9%) used for LTTM production were purchased from R&M Chemicals and Sigma Aldrich, respectively. For the synthesis of catalyst, powdered activated carbon was bought from R&M Chemicals, while the precursor copper nitrate trihydrate (>99.5%) was from Merck. High-purity N_2 and H_2 gases were supplied by Linde Malaysia, and chromatography grade methanol was from Sigma Aldrich.

2.2 Synthesis of LTTMs

The synthesis procedure and conditions of LTTM were in accordance to our previous study (Lim, Rashidi, Cheah, & Abdul Manaf, 2023). A 1:1 mass ratio was employed for the preparation. In a standard experiment, 100 g of ChCl was weighed into a clean beaker, followed by the gradual addition of 100 g of malic acid, which was mixed thoroughly with ChCl to produce a uniform solid powder mixture. The mixture was then heated in an oil bath at 90 °C with continuous stirring. Initially, manual stirring with a glass rod was used to help the mixture melt into a viscous liquid. Once melted, stirring was continued using a magnetic stirrer for at least 6 hours until the LTTM became clear. Example of images of appearances changes during the stirring were shown in Fig. 1. To eliminate trapped air bubbles, the LTTM underwent sonication. Finally, it was stored in an air-tight container at a chilled temperature of 5 °C for future use.

2.3 Dilute acid hydrolysis of bamboo

The collected bamboo was first ground into fine particles (<250 μ m) and dried in an oven (UF110, Memmert) at 105 °C for a minimum of 12 hours. A 0.5 M $\rm H_2SO_4$ solution was used for bamboo hydrolysis. The process was carried out in a 500 mL PTFE-lined steel autoclave reactor (TOPT-HT500, KSFE Malaysia). Before the experiment, the bamboo sample was dried again at 105 °C for at least 12 hours if it was stored for an extended period of time. Subsequently, 40 g of bamboo and 400

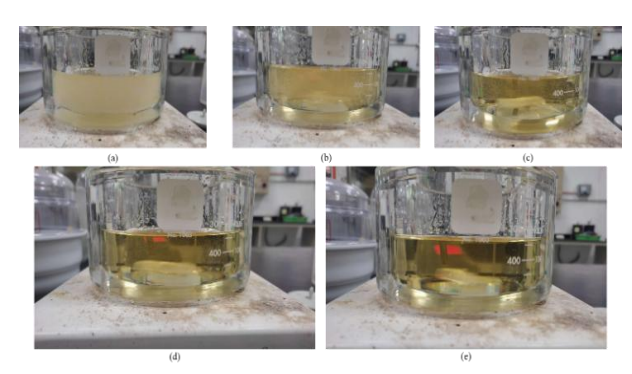


Fig. 1 Changes in LTTM mixture from (a) 4 hours, (b) 5 hours, (c) 6 hours, (d) 7 hours, and (e) 8 hours

mL of 0.5 M $\rm H_2SO_4$ were placed into the PTFE liner and thoroughly mixed using a magnetic stirrer for 1 hour to ensure the bamboo powder was in good contact with acid solution. The PTFE liner was then sealed and secured inside the steel autoclave. The hydrolysis process was performed at 140 °C for 2 hours in the drying oven. After cooling to room temperature, the product was filtered using vacuum pump, and the liquid hydrolysate was stored in a glass bottle at -5 °C to prevent undesired side reactions and degradation.

2.4 Cu/AC catalyst synthesis

Wet incipient impregnation method was employed in the synthesis of Cu/AC catalyst (Cheah et al., 2020). The nominal loading of copper metal targeted was 10 wt.% (e.g., 1g of Cu on 9g of activated carbon, forming 10g of catalyst). To achieve this, 3.802g of Cu(NO₃)₂·3H₂O was used with 9g of activated carbon, and the numbers can be multiplied accordingly depending on the desired batch size. The activated carbon was dried at 105 °C overnight prior to the experiment, while the Cu(NO₃)₂·3H₂O was not dried in prior and used as received, due to potential of thermal decomposition of this crystal to copper hydroxy nitrate [Cu₂(OH)₃NO₃] at above 80 °C (Kon Ryu et al., 2004). Next, 3.802 g of Cu(NO₃)₂·3H₂O was measured in a clean beaker, and roughly 50 mL of distilled water was added directly into the beaker. Then, the solution was stirred vigorously at 300 RPM using magnetic stirrer for at least 2 hours to fully dissolve the Cu(NO₃)₂·3H₂O. After that, the solution was treated with sonication for 0.5 hour for greater dissipation of the dissolved Cu(NO₃)₂·3H₂O (Cheah et al., 2020). Then, the treated solution was placed back to the magnetic stirrer and continued stirring at 300 RPM. Activated carbon was then slowly and gradually added into the solution with a clean spatula. Due to the slight hydrophobicity of activated carbon, some chunks of activated carbon may be formed on the solution surface that refused to be wet. Spatula was used to manually break down the floating chunks and then rinsed with slight amount of distilled water to transfer the activated carbon sticked on the spatula into the solution. The wall of the beaker was also rinsed slightly with distilled water to transfer the attached fine activated carbon powder into the solution. After that, the solution was stirred for another 2 hours before the hot plate was turned on to 80 °C and left ageing overnight for at least 12 hours. Lastly, the aged catalyst was further dried in oven at 80 °C for 24 hours to obtained dried Cu(NO₃)₂ impregnated catalyst. To remove the nitrate anion from the impregnated crystal, consecutive calcination and reduction treatments were performed. The two processes were performed in-situ using a stainless-steel autoclave reactor as shown in Fig. 2. The impregnated catalyst was loaded in a clean ceramic crucible and placed into the autoclave.

A K-type thermocouple was inserted into the enclosed autoclave to monitor the reaction temperature. Before heating up, the system was purged with high purity N_2 gas at 100 mL/min for at least 10 mins at room temperature to establish an inert environment. After that, the N_2 gas flow was reduced to

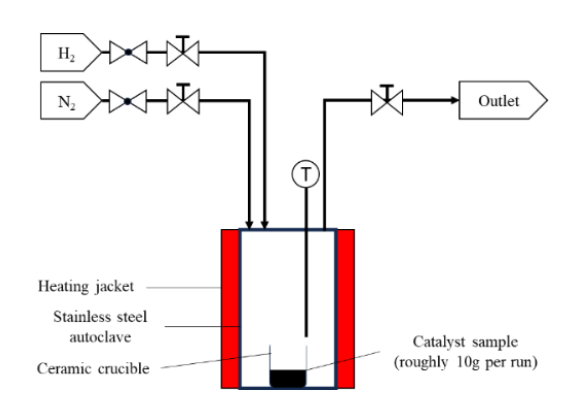


Fig. 2 Schematic diagram of hydrogen stainless-steel autoclave reactor

25 mL/min and the heater was turned on with set point at 450 °C to start with the calcination process. The process lasted for 2 hours after the set point was reached. Following that, the gas was changed to H_2 with similar flowrate while maintaining the temperature at 450 °C to initiate the reduction process, which also lasted for 2 hours. Lastly, the system was purged again with N_2 gas to remove the H_2 and subsequently cooled down to room temperature before the retrieval of Cu/AC product.

2.5 Microwave assisted DMF synthesis and parametric study

The microwave synthesis reactor (Dixson, Malaysia) used was as shown in Fig. 3. The reactor can provide an output of up to 3000 W. The reaction temperature was fixed at 120 °C as obtained in previous study (Lim, Rashidi, Cheah, & Abdul Manaf, 2023). Three factors were studied: reaction time, LTTMto-hydrolysate ratio, and Cu/AC catalyst loading, which were typical variables in DMF synthesis (Binder & Raines, 2009; De et al., 2012; Liu & Zhang, 2016; Wei et al., 2016). The CCRD was employed in this parametric and optimization study with the assistance from Design Expert® v12 (Stat-Ease, USA) (Table 1). The software was also used to undertake analysis of variance (ANOVA) in determining the significant factors as well as constructing the regression model from the experimental data. Before the experiment, both the LTTM and hydrolysate were thoroughly mixed at different ratios as per the CCRD using magnetic stirring at 300 RPM until a uniform phase was achieved. A 30 g portion of the mixture was then transferred into a two-neck round-bottom flask, added with stipulated amount of Cu/AC catalyst depending on the catalyst loading in CCRD. After that, the loaded flask was set up in the microwave reactor as illustrated in Fig. 3. The flask's top neck was connected to a condenser with a constant supply of chilled water at 15 °C, while the side neck was fitted with a K-type thermocouple linked to the control panel for temperature monitoring and regulation. A magnetic stirring bar was also added to the flask to maintain stirring during the reaction. Once the setup was complete, the experiment commenced following

Table 1 Independent factors and design levels.

Factors	Unit	Levels					
		-1.68	-1	0	+1	+1.68	
Time	Min	0.98	2	3.5	5	6.02	
LLTM ratio	g/g hydrolysate	0	0.81	2	3.19	4	
Catalyst loading	Wt.%	0	1.01	2.5	3.99	5	

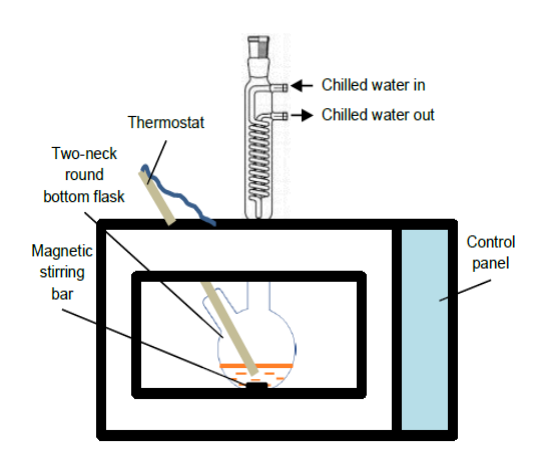


Fig. 3 Schematic diagram of 103L microwave synthesis reactor used (Lim, Rashidi, Cheah, & Abdul Manaf, 2023)

the specified temperatures and durations in CCRD. After the reaction, the product was left in the oven with the condenser operational to minimize water vapor loss until it cooled to room temperature. Subsequently, the liquid product was collected via vacuum filtration to remove the solid Cu/AC catalyst and stored at -5 $^{\circ}$ C in vial for further characterization.

2.6 Characterization and quantification

2.6.1 Quantification of glucose content

The glucose contents in the hydrolysate and products were analysed using High-performance liquid chromatography (HPLC) coupled with reflective index detector (RID) (Shimadzu LC20A, Japan), based on the method reported (Abdul Manaf et al., 2023). Before the analysis, the samples were neutralized to a pH range of 5–7 using 1.0 M NaOH solution, with the volume of NaOH added recorded as the dilution factor. The neutralized samples were then filtered through a 0.45 µm PTFE syringe filter, after which they were prepared for analysis. The analysis employed an Agilent InfinityLab Poroshell EC-C18 column (4.6 \times 250 mm, 4 μ m). The mobile phase consisted of 80% acetonitrile and 20% deionized water (by volume), which was filtered and degassed before use. The flow rate of the mobile phase was set to 1.2 mL/min, with the column oven maintained at 30 °C. A sample injection volume of 5 µL was used. Quantification of glucose content was achieved through an external calibration curve that correlated the peak area with the actual glucose concentration. The glucose conversion can then be calculated using Equation 1 (Ayele et al., 2014).

Glucose conversion (%) = $\frac{\text{moles of glucose in sample-moles of glucose in product}}{\text{moles of glucose in sample}} \times 100\%$ (1)

2.6.2 Quantification of DMF content

Quantifications of DMF in products were performed using Gas Chromatography coupled with Flame Ionisation Detector (GC-FID) (Agilent 7820A) based on method reported in literature (Hu et al., 2014). The column used was Agilent HP-5 (0.32 mm x 30 m, 0.25 μ m). A 99.9999% high-purity helium was used as the carrier gas with a flowrate of 1 mL/min. The injector temperature was maintained at 250 °C, while the FID temperature was 270 °C. The injection volume used was 1 μ L

with a split ratio of 1:10. Prior to injection, the product sample was diluted with chromatography-grade methanol at a dilution factor of 5. The injector was also triple-rinsed with chromatography-grade methanol before drawing the sample to avoid contaminations. Similar to glucose, the quantification of DMF was done using external calibration curve that correlated the peak area and the actual DMF concentration. The DMF yield can then be calculated using Equation 2.

DMF yield%=
$$\frac{\text{moles of DMF in product}}{\text{moles of glucose in sample}} \times 100 \%$$
 (2)

2.6.3 Characterization of bamboo biomass

Ultimate analysis of the bamboo biomass sample was conducted by using CHNS elemental analyser (VarioMicro, Elementar). The compositions of elemental carbon, hydrogen, nitrogen, and sulphur were measured, while oxygen content was obtained by calculating the difference. In the CHNS analyser, the temperature of the furnace was 1000 °C, followed by reduction at 650 °C. Prior to the run, the equipment was calibrated using sulphanilamide. In addition, the compositional analysis of bamboo was performed in accordance with the Technical Association of the Pul and Paper Industry (TAPPI) standards. The extractives, α -cellulose, holocellulose, and lignin contents of bamboo were measured with respective TAPPI standard test methods. Specifically, the test methods were T204, T203, T249, and T222, respectively (Wahab et al., 2013).

2.6.4. Characterization of LTTM

Thermal stability of the LTTM was measured via thermogravimetric analysis (TGA) (STA6000, Perkin Elmer). The thermal analysis was conducted within a temperature range of 20 °C to 250 °C, with a heating rate of 10 °C/min. A sample size of 10 mg loaded in an alumina pan was used for each run. Air was used as the carrier gas with a flow rate of 50 mL/min. On the other hand, the density of LTTM at 25 °C was measured using a densitometer (DA-645, KEM).

2.6.5. Characterization of Cu/AC catalyst

Reduction properties of the calcined CuO/AC catalyst was determined by using the temperature programming reduction (TPR) method via TPDRO 1100 (Thermo Scientific). Prior to analysis, the system was purged with N2 for 5 minutes, followed by sample pretreatment at an elevated temperature of 150 °C for 30 minutes in N2 atmosphere. Once ready, the TPR commenced using 5.05% H₂ in N₂ at a flowrate of 25 mL/min. The temperature range analysed was 50-950 °C with a fixed heating rate of 10 °C/min. Besides, X-ray diffraction (XRD) was employed to analyse the crystallinity and structure of the catalyst using X'pert3 Powder diffractometer (Malvern Panalytical). The voltage and current used were 45 kV and 40 mA, respectively. The scanning angle was $2\theta = 10-80$ deg, with a step size of 0.04 deg/step and exposure time of 30 s/step. The anode was made of copper, utilizing K-Alpha1 and K-Alpha2 emissions. Further, surface morphology of the calcined and reduced Cu/AC catalyst was determined via Scanning Electron Microscopy coupled with Energy Dispersive X-ray (SEM-EDX). The equipment used was Zeiss EVOLS15. Prior to the analysis, the Cu/AC samples were dried in an oven at 105 °C overnight, followed by gold coating using a sputter immediately before loading into the SEM-EDX machine. The magnification observed was 500x with an energy of 10 keV for SEM, while it was 25 keV for EDX.

Table 2Elemental analysis and compositional analysis based on TAPPI standard method of bamboo

Elemental a	nalysis	Compositional analysis			
Item	Value	Item	Value		
Carbon	43.070%	Extractive	1.92%		
Hydrogen	4.648%	α-cellulose	37.31%		
Nitrogen	2.530%	Hemicellulose	22.75%		
Sulphur	0.058%	Lignin	13.29%		
Oxygen*	49.694%				

^{*} Calculated by difference

3. Results and discussion

3.1 Characteristics of bamboo biomass

The properties of bamboo biomass from the elemental and compositional analysis are presented in Table 2. The elemental analysis shows that the bamboo is mainly comprised of organic matters, evidenced by high carbon, hydrogen, as well as oxygen contents. Further, presence of nitrogen refers to nitrogenous biomolecules such as proteins, while the sulphur content is negligible. Meanwhile, the compositional analysis shows a high value of cellulose content in the bamboo, indicating potential of high glucose content in the hydrolysate. Indeed, Bandgar et al. (2022) reported that the biomass with high cellulose fraction is suitable to be utilized for biochemical and biofuel synthesis, at which the hydrolysis method could convert them to fermentable sugar. Compared to other biomass, cellulose content of bamboo is competitive with other lignocellulosic biomass, such as rice straw (~32.15%), corn stover (~40.67%), and sugarcane bagasse (~35.8%) (Bandgar et al., 2022; Saravanan et al., 2022).

3.2 Characteristics of LTTMs

Fig. 4 shows the trend of mass changes of LTTM in the air condition. Here, the mass changes indicate the thermal stability of LTTM during the microwave-assisted synthesis process later, where it was being exposed in an air atmosphere at elevated temperature. It was found that at the reaction temperature of 120 °C, the LTTM experienced a mass loss of about 7.30%. Thereby, this LTTM solvent is considered thermally stable at such reaction temperature in air atmosphere. Furthermore, the density of the LTTM at 25 °C was determined to be 1.27966 g/cm³. This value is comparable with reported literature values of 1.2731 g/cm³ (Abdul Manaf et al., 2023) and 1.278 g/cm³ (Al-Risheq *et al.*, 2021).

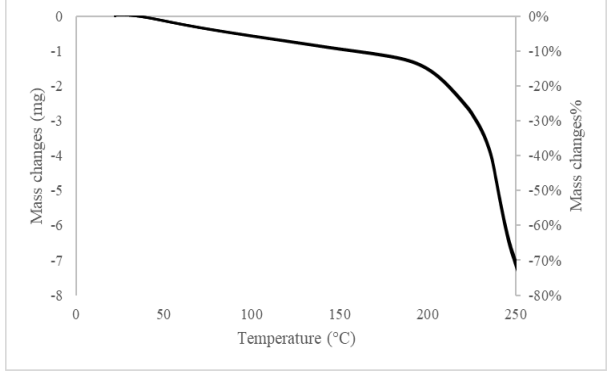


Fig. 4 Mass changes from TGA of LTTM in air condition

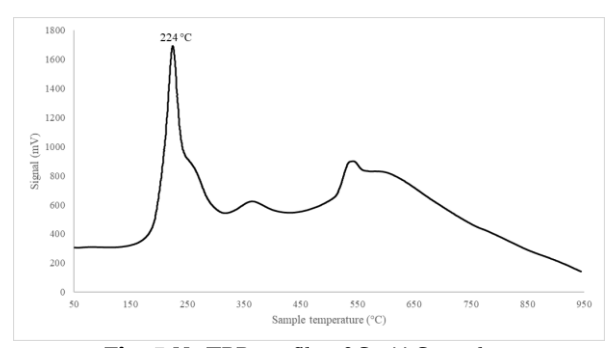


Fig. 5 H₂-TPR profile of Cu/AC catalyst

3.3 Characteristics of Cu/AC catalyst

3.3.1 TPR profile of calcined Cu/AC catalyst

The profile of the catalyst in H₂-TPR is illustrated in Fig. 5. Commonly, reduction of CuO occurs at temperature of 200-300 °C (Chary et al., 2004). Based on Fig. 5, a sharp peak at 224 °C stands out, which corresponds to the one-step reduction of CuO to Cu. The reduction temperature is considerably lower than the reported values in literatures for activated carbon supported copper, for example 294 °C (Anuar et al., 2014) and 270 °C (Seguel et al., 2020). Here, both size and dispersion of copper particles play a significant role. Larger particles tend to reduce at higher temperature due to reduced specific surface area for the reduction process (Agrell, 2003), whereas well-dispersed small CuO particles lead to decreased reduction temperatures (Flores et al., 2011). Similar observations were achieved by Chary et al. (2004), whereby catalysts with Cu loading of 5% and above showcased two distinct peaks for dispersed and bulk CuO particles. Further, a small peak at 360 °C as shown in Fig. 5 may indicate the reduction of bulky CuO particles. Furthermore, beyond 450 °C, there is an increase in the H₂ consumption, which is contributed by the oxygen and organic compounds present on the activated carbon (as received) used in this study. Therefore, it is evident that the reduction temperature of 450 °C used in the catalyst preparation is sufficient to reduce the CuO particles to metallic Cu while causing a minimal change to the activated carbon structures.

3.3.2 XRD of Cu/AC catalyst

The XRD spectrum of the Cu/AC catalyst used in this study is shown in Fig. 6. The broad peak at $2\theta = 25^{\circ}$ is attributed to the activated carbon support used with the presence of C(002) plane (Ling et al., 2015; Shelepova et al., 2017). A tiny peak at $2\theta =$

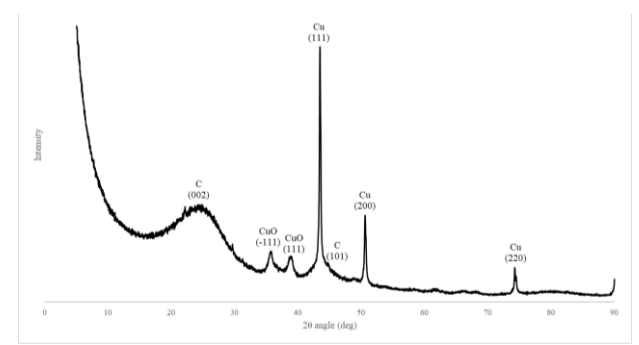


Fig. 6 XRD spectrum of Cu/AC catalyst

44° is also contributed by the C(101) plane, with overlapping with crystalline reflections from copper at $2\theta=43.4^\circ$ (Giannousi et al., 2013; Ling et al., 2015). Subsequently, the peaks at $2\theta=43.4^\circ$, 50.4° , and 74.0° are results from the (111), (200), and (220) planes from Cu^0 face-centred cubic (f.c.c.) crystalline structure, respectively (Giannousi *et al.*, 2013; Viar *et al.*, 2022). This further supported that the CuO particles on the calcined catalyst has successfully been reduced, albeit not being entirely reduced. The two small peaks at $2\theta=35.94^\circ$ and 39.17° are contributed by the (-111) and (111) planes of CuO crystals, indicating the residue from H_2 reduction or the re-oxidation during the storage (Hosseini *et al.*, 2021).

3.3.3 SEM-EDX of Cu/AC catalyst

To further verify the presence of Cu in the synthesized catalyst, surface morphology of the calcined Cu/AC catalyst has been analysed. Referring to Fig. 7, the synthesized catalyst exhibits a rough structure with noticeable porosity on the exterior surface. Referring to Maiyalagan and Scott (2010), formation of larger rough surface particles are contributed by an agglomeration of the Cu/AC. Further, EDX spectrum (Fig. 8) proves that Cu/AC

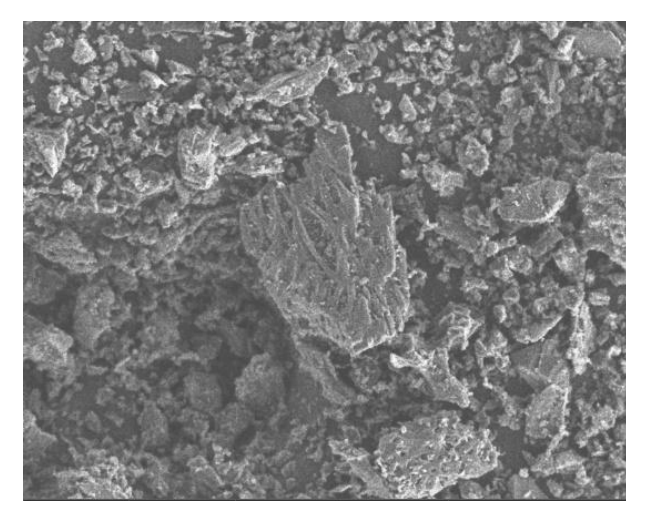


Fig. 7 SEM image of Cu/AC catalyst at 500x magnification

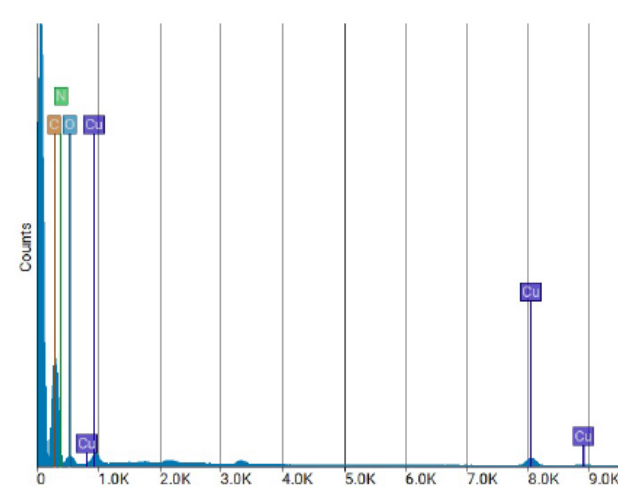


Fig. 8 EDX spectra of Cu/AC catalyst

has a certain content of Cu compound in the structure, implying successful loading of Cu particles. Specifically, the synthesized Cu/AC catalyst is comprised of the following: 61.76 wt.% C, 27.72 wt.% N, 1.74 wt.% Cu, and balanced with O. While C content is plausibly due to the carbon content in the activated carbon support, Cu and N content originate from the precursor materials (i.e., copper nitrate). Further, O content is likely due to the presence of CuO as residues from reduction process and unwanted oxidation during storage. This observation is also agreed with the XRD result obtained where crystalline structure of CuO was found. Nevertheless, it is important to note that the EDX composition is based on a localized spot analysis and may not fully represent the entire sample.

3.4 CCRD results

The results of the 20 runs generated from CCRD are presented in Table 3. Among these three factors, LTTM ratio is observed to possess the greatest effects toward DMF yield. In Run 1, 2, 3, and 6 where the LTTM ratios were constant at 0.81, the DMF yields lingered below 5%. When no LTTM was used as shown in Run 5, the DMF yield dropped to no more than 0.25%. Vice versa, the DMF yields were much higher when more LTTM was mixed in the reactant. In fact, the three highest DMF yields were achieved with LTTM ratio of 3.19 and 4.00 at Run 11, 13, and 14, reaching up to 17.37%. On the other hand, both Cu/AC catalyst loading and reaction time seem to have minimal effects towards the DMF yield. In Run 5 where no LTTM was present, having 2.5% Cu/AC catalyst did not lead to higher DMF yield. Thus, from a glance, the most influential factor is the LTTM ratio in the system. Besides, products from all 20 runs were analysed for the remaining glucose content upon the accomplishment of microwave assisted synthesis. In all samples, no glucose was detected via the HPLC, implying that the glucose leftover in the products was well below the detection limit of the analytical machine. Following that, it was assumed that all the glucose content in the bamboo hydrolysate was wholly consumed in the reaction.

3.4.1 ANOVA and statistical analytical results of CCRD

ANOVA is a statistical tool to analyse and determine the significances of each factor, most commonly via the p-values. In this study, a p-value of <0.05 indicates that the particular factor is significant. From Table 4, it was found that the quadratic regression model, LTTM ratio, as well as catalyst ratio were

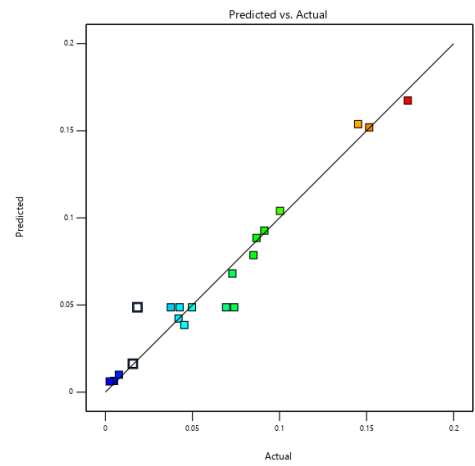


Fig. 9 Plot between the predicted data and actual experiment data of the CCRD

Table 3CCRD result of microwave assisted DMF synthesis

Run	Time (min)	LTTM ratio (g/g hydrolysate)	Catalyst loading (wt.%)	Exp. DMF yield% (mol/mol glucose)	Pred. DMF yield% (mol/mol glucose)
1	2.00	0.81	3.99	0.4983%	0.6455%
2	2.00	0.81	1.01	1.5792%	1.6273%
3	5.00	0.81	1.01	4.2025%	4.2243%
4	6.02	2.00	2.50	10.0306%	10.4035%
5	3.50	0.00	2.50	0.2486%	0.6140%
6	5.00	0.81	3.99	4.5334%	3.8552%
7	5.00	3.19	3.99	9.1313%	9.2708%
8	3.50	2.00	2.50	3.7589%	4.8702%
9	3.50	2.00	5.00	0.7780%	1.0008%
10	3.50	2.00	2.50	1.8411%	4.8702%
11	5.00	3.19	1.01	15.1530%	15.1938%
12	2.00	3.19	3.99	8.6810%	8.8471%
13	2.00	3.19	1.01	14.5163%	15.3828%
14	3.50	4.00	2.50	17.3690%	16.7349%
15	0.98	2.00	2.50	8.5043%	7.8634%
16	3.50	2.00	0.00	7.2982%	6.8071%
17	3.50	2.00	2.50	4.9777%	4.8702%
18	3.50	2.00	2.50	6.9339%	4.8702%
19	3.50	2.00	2.50	7.4016%	4.8702%
20	3.50	2.00	2.50	4.2651%	4.8702%

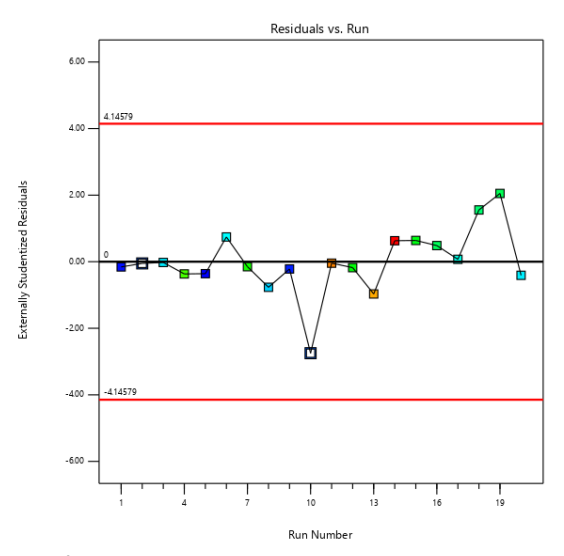


Fig. 10 Externally studentized residuals plot

significant with p-value of <0.0001 and 0.0021, respectively. In addition, the R^2 value was found to be 0.9481 and the lack of fit was not significant, indicating great fits between the data and the regression model. This was also supported by the plot of predicted vs actual data points shown in Fig. 9. From the externally studentized residuals plot in Fig. 10, it showed that all of the experiment data points from the CCRD fell within the limit and no data point was considered as outlier. Thus, the quadratic regression model constructed in this study was considered to be reliable, fitting, and completed. The quadratic regression model equation for this CCRD is given in Equation 3, where

term A, B, and C refers to time, LTTM ratio, and catalyst ratio, respectively, as mentioned in Table 4.

DMF Yield% =
$$2.9406 - 3.5772A + 3.5563B +$$
 (3)
 $0.9411C - 0.3902AB + 0.0684AC - 0.87849BC +$
 $0.6699A^2 + 0.9498B^2 - 0.1546C^2$

For the quadratic factors, BC, A^2 , and B^2 were significant, whereby A is the reaction time, B is LTTM ratio, and C is the catalyst ratio. The terms A^2 and B^2 imply that the reaction time and LTTM ratio have quadratic effects toward the DMF yield,

Table 4Results of ANOVA and quadratic regression from the CCRD runs

Source	Sum of Squares	df	Mean Square	F-value	p-value	Remark
Model	0.0441	9	0.0049	20.30	< 0.0001	significant
A-Time	0.0008	1	0.0008	3.23	0.1026	· ·
B-LTTM ratio	0.0314	1	0.0314	130.11	< 0.0001	significant
C-Catalyst loading	0.0041	1	0.0041	16.87	0.0021	significant
AB	0.0004	1	0.0004	1.61	0.2334	
AC	0.0000	1	0.0000	0.0778	0.7859	
BC	0.0015	1	0.0015	6.39	0.0299	significant
A^2	0.0033	1	0.0033	13.58	0.0042	significant
B^{2}	0.0026	1	0.0026	10.81	0.0082	significant
C ²	0.0002	1	0.0002	0.6974	0.4232	
Residual	0.0024	10	0.0002			
Lack of Fit	0.0003	5	0.0001	0.1240	0.9806	not significant
Pure Error	0.0021	5	0.0004			
Cor Total	0.0465	19				
Std. Dev.	0.0155					
Mean	0.0659		R²		0.9481	
C.V. %	23.58		Adjusted R ²		0.9014	
Adeq. Precision	14.6825		Predicte	ed R ²	0.8890	

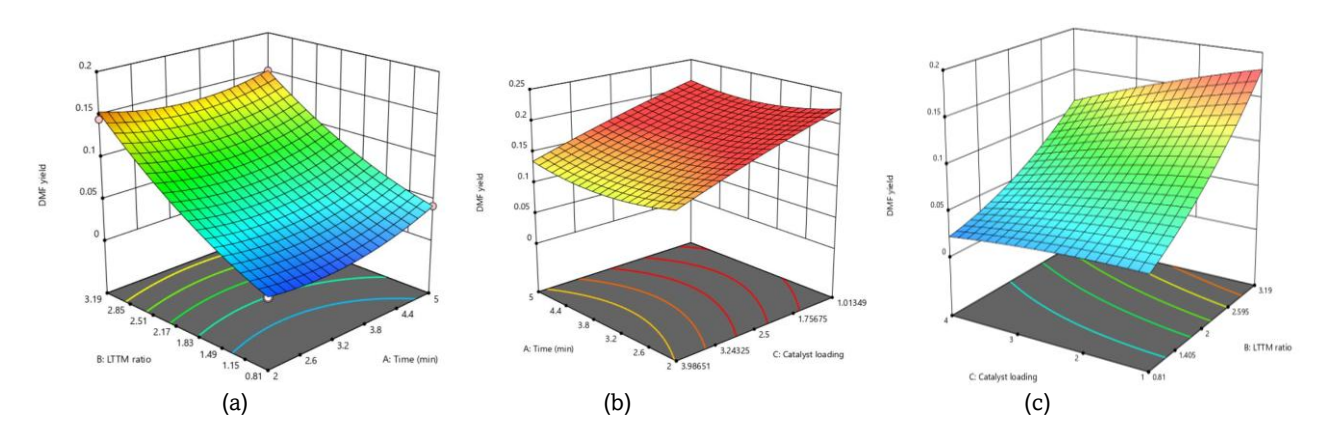


Fig. 11 3D surface plot for (a) time and LTTM ratio at catalyst loading = 1 wt.%, (b) time and catalyst loading at LTTM ratio = 4, and (c)

LTTM ratio and catalyst loading at time = 1 min.

which can be observed from Fig. 11. In Fig. 11a and Fig. 11b, it is clear that reaction time has a U-shaped curve towards the DMF yield, with highest yields at both ends, whereas the curvatures of LTTM ratio are subtle in Fig. 11a and Fig. 11c, showing a slightly curved slope. Comparatively, catalyst loading presented straight lines in both Fig. 11b and Fig. 11c. The significant quadratic factors of BC illustrate that there is a synergistic relationship between the LTTM ratio and catalyst loading. This relationship can be reflected in Fig. 11c showing the 3D surface plot between the two factors. At low LTTM ratio (e.g., 0.81), the changes in DMF yield along the catalyst loading axis appeared to be stagnant. This may be due to insufficient amount of intermediate HMF produced, resulted by the lack of LTTM to dissolute and facilitate the reaction (Chen et al., 2020). In contrast, at the high LTTM ratio of 3.19, the DMF yield was greatly affected by the catalyst loading, where the highest yield occurred at the lowest catalyst loading of 1%. Esteves et al. (2020) studied and proposed a potential reaction pathway of HMF to DMF on copper-based catalysts, where in the presence of water and H2 (or donor), the DMF may be further hydrogenated into various by-products, namely 1,4-pentadie-3ol and hexanol. Therefore, it can be deduced that an excessive

amount of Cu/AC catalyst in this study led to over-hydrogenolysis of the DMF, indirectly reducing the yields.

3.4.2 Optimization from CCRD

With the established quadratic regression model, the optimum point for the maximum DMF yield was determined using the software Design Expert v12®. A reaction time of 1 min, LTTM ratio of 4, and Cu/AC catalyst loading of 1% was determined to be the optimum point in this study, with expected DMF yield of 25.60 mol%. Subsequently, experimental validation runs were performed to verify the validity of the predicted data. Triplicate runs at the optimum point resulted in a 21.28 ± 0.77 mol% of DMF, with a 4.32 mol% difference with the predicted yield. This suggested that the quadratic regression CCRD model obtained was accurate and experimentally validated. Overall, the findings are promising since no previous study has explored the direct one-pot conversion of biomass-derived glucose or hydrolysate to DMF. Insyani et al. (2017) did achieve a notable DMF yield of 45.30 mol% using a similar approach. Nevertheless, utilization of high-purity commercial glucose could make the process more expensive and less practical for large-scale applications. Not

only that, the findings are also comparable to conventional two-stage processes; De et al. (2012) produced the DMF synthesis from corn stover using ionic liquid and 1-butanol solvents, and obtained a combined DMF yield of 9%.

4. Conclusion

Microwave-assisted direct production of DMF is achieved in presence of the LTTM made from ChCl and malic acid, and the Cu/AC catalyst. Thermal stability test on the LTTM shows that the green solvent experiences a minimal mass loss of less than 10% at the reaction temperature of 120 °C. The Cu/AC catalyst is synthesized via wet incipient impregnation followed by posttreatment of calcination and reduction, where it is found that the Cu/AC has been successfully reduced at the calcination and reduction temperature of 450 °C, with some residues of copper oxide on the activated carbon support. Subsequently, this catalyst is used in the production of DMF from the bamboo hydrolysate. The CCRD study discovers that the LTTM and catalyst loading hold a significant role in affecting the DMF yield. Furthermore, there is a synergistic relationship between LTTM and catalyst loading due to the amount of intermediate HMF produced and the competing over-hydrogenolysis of DMF into undesired products. Finally, the quadratic regression model obtained is significant with great fits, where the corresponding R² value acquired is 0.9481. Further, the predicted optimum point from this quadratic model is 25.60 mol% of DMF yield. Triplicate experimental validation runs provided with 21.28 \pm 0.77 mol% of DMF yield, further indicating the accuracy of the model. Thus, it is concluded that the system established in this study is capable in producing DMF from bamboo hydrolysate, with great predictability using quadratic regression.

Acknowledgments

The authors would like to acknowledge the Ministry of Higher Education Malaysia for providing the support and awarding the Higher Institution of Centre of Excellence (HICoE) status to the Centre of Biofuel and Biochemical (CBBR), Universiti Teknologi PETRONAS.

Author Contributions: H.Y.L.; methodology, formal analysis, original draft, N.A.R.; supervision, writing—review and editing, S.Y.; writing—review and editing. All authors have read and agreed to the published version of the manuscript.

Funding: This research was funded by the Yayasan Universiti Teknologi PETRONAS (Project no: RG2022-0755).

Conflicts of Interest: The authors declare no conflict of interest.

References

- Abdul Manaf, A. S., Mostapha, M., Ameen, M., Yusup, S., & Amran, N. A. (2023). Optimization Study of Glucose Synthesis to 5-Hydroxymethylfurfural (5-HMF) by Using Low Transition-Temperature Mixtures (LTTM). Catalysts, 13(5). https://doi.org/10.3390/catal13050829
- Agarwal, B., Kailasam, K., Sangwan, R. S., & Elumalai, S. (2018). Traversing the history of solid catalysts for heterogeneous synthesis of 5-hydroxymethylfurfural from carbohydrate sugars:

- A review. Renewable and Sustainable Energy Reviews, 82, 2408-2425. https://doi.org/10.1016/j.rser.2017.08.088
- Agrell, J. (2003). Production of hydrogen from methanol over Cu/ZnO catalysts promoted by ZrO2 and Al2O3. *Journal of Catalysis*, 219(2), 389-403. https://doi.org/10.1016/s0021-9517(03)00221-5
- Al-Risheq, D. I. M., Nasser, M. S., Qiblawey, H., Ba-Abbad, M. M., Benamor, A., & Hussein, I. A. (2021). Destabilization of stable bentonite colloidal suspension using choline chloride based deep eutectic solvent: Optimization study. *Journal of Water Process Engineering*, 40. https://doi.org/10.1016/j.jwpe.2020.101885
- Anuar, A., Yakub, I., Mohamed Sutan, N., Hipolito, C. N., & Taufiq-Yap, Y. H. (2014). Temperature-Programmed Reduction of Copper-Manganese Catalysts Derived from Biomass Activated Carbon. Journal of Applied Science & Process Engineering, 1(1), 28-38. https://doi.org/10.33736/jaspe.157.2014
- Ayele, L., Dadi, G., Mamo, W., Chebude, Y., & Diaz, I. (2014). Conversion of glucose into platform chemicals using aluminophosphates (SAPO-5 and MeAPO-5) in [BMIM]Cl ionic liquid. *Bulletin of the Chemical Society of Ethiopia*, 28(1). https://doi.org/10.4314/bcse.v28i1.6
- Bandgar, P. S., Jain, S., & Panwar, N. L. (2022). A comprehensive review on optimization of anaerobic digestion technologies for lignocellulosic biomass available in India. *Biomass and bioenergy*, 161. https://doi.org/10.1016/j.biombioe.2022.106479
- Binder, J. B., & Raines, R. T. (2009). Simple Chemical Transformation of Lignocellulosic Biomass into Furans for Fuels and Chemicals. *Journal of the American Chemical Society*, 131(5), 1979-1985. https://doi.org/10.1021/ja808537j
- Cereda, M. P. (2024). Chapter 5 Starch hydrolysis: physical, acid, and enzymatic processes. In M. P. Cereda & O. F. Vilpoux (Eds.), Starch Industries: Processes and Innovative Products in Food and Non-Food Uses (pp. 75-113). Academic Press. https://doi.org/https://doi.org/10.1016/B978-0-323-90842-9.00016-9
- Chakraborty, D., & Mondal, N. K. (2018). Hypertensive and toxicological health risk among women exposed to biomass smoke: A rural Indian scenario. *Ecotoxicology and Environmental Safety*, *161*, 706-714. https://doi.org/10.1016/j.ecoenv.2018.06.024
- Chary, K. V. R., Seela, K. K., Sagar, G. V., & Sreedhar, B. (2004). Characterization and Reactivity of Niobia Supported Copper Oxide Catalysts. *The Journal of Physical Chemistry B*, 108(2), 658-663. https://doi.org/10.1021/jp035738s
- Cheah, K. W., Taylor, M. J., Osatiashtiani, A., Beaumont, S. K., Nowakowski, D. J., Yusup, S., Bridgwater, A. V., & Kyriakou, G. (2020). Monometallic and bimetallic catalysts based on Pd, Cu and Ni for hydrogen transfer deoxygenation of a prototypical fatty acid to diesel range hydrocarbons. *Catalysis Today*, 355, 882-892. https://doi.org/10.1016/j.cattod.2019.03.017
- Chen, W. C., Lin, Y. C., Chu, I. M., Wang, L. F., Tsai, S. L., & Wei, Y. H. (2020). Feasibility of enhancing production of 5-hydroxymethylfurfural using deep eutectic solvents as reaction media in a high-pressure reactor. *Biochemical Engineering Journal*, 154. https://doi.org/10.1016/j.bej.2019.107440
- De, S., Dutta, S., & Saha, B. (2012). One-pot conversions of lignocellulosic and algal biomass into liquid fuels. *ChemSusChem*, 5(9), 1826-1833. https://doi.org/10.1002/cssc.201200031
- Deivayanai, V. C., Yaashikaa, P. R., Senthil Kumar, P., & Rangasamy, G. (2022). A comprehensive review on the biological conversion of lignocellulosic biomass into hydrogen: Pretreatment strategy, technology advances and perspectives. *Bioresource technology* 365. https://doi.org/10.1016/j.biortech.2022.128166
- Endot, N. A., Junid, R., & Jamil, M. S. S. (2021). Insight into biomass upgrade: A review on hydrogenation of 5-hydroxymethylfurfural (hmf) to 2,5-dimethylfuran (dmf). *Molecules*, 26. https://doi.org/10.3390/molecules26226848
- Esteves, L. M., Brijaldo, M. H., Oliveira, E. G., Martinez, J. J., Rojas, H., Caytuero, A., & Passos, F. B. (2020). Effect of support on selective 5-hydroxymethylfurfural hydrogenation towards 2,5-dimethylfuran over copper catalysts. *Fuel*, 270. https://doi.org/10.1016/j.fuel.2020.117524
- Flores, J. H., Peixoto, D. P. B., Appel, L. G., de Avillez, R. R., & Silva, M. I. P. d. (2011). The influence of different methanol synthesis

- catalysts on direct synthesis of DME from syngas. *Catalysis Today*, 172(1), 218-225. https://doi.org/10.1016/j.cattod.2011.02.063
- Giannousi, K., Avramidis, I., & Dendrinou-Samara, C. (2013). Synthesis, characterization and evaluation of copper based nanoparticles as agrochemicals against Phytophthora infestans. *RSC Advances*, 3(44), 21743-21752. https://doi.org/10.1039/C3RA42118J
- Gomes, G. R., & Pastre, J. C. (2020). Microwave-assisted HMF production from water-soluble sugars using betaine-based natural deep eutectic solvents (NADES) [10.1039/C9SE01278H]. Sustainable Energy & Fuels, 4(4), 1891-1898. https://doi.org/10.1039/C9SE01278H
- He, J., Peng, J., Ling, R., & Wang, J. (2024). Recent Progress on the Production of Liquid Fuel 2,5-Dimethylfuran via Chemoselective Hydrogenolysis Biomass-Derived 5-Hydroxymethylfurfural. Catalysts, 15(1). https://doi.org/10.3390/catal15010031
- Hoang, A. T., Nižetić, S., & Ölçer, A. I. (2021). 2,5-Dimethylfuran (DMF) as a promising biofuel for the spark ignition engine application: A comparative analysis and review. *Fuel*, 285. https://doi.org/10.1016/j.fuel.2020.119140
- Hosseini, M., Chin, A. W. H., Behzadinasab, S., Poon, L. L. M., & Ducker, W. A. (2021). Cupric Oxide Coating That Rapidly Reduces Infection by SARS-CoV-2 via Solids. *ACS Appl Mater Interfaces*, 13(5), 5919-5928. https://doi.org/10.1021/acsami.0c19465
- Hu, L., Tang, X., Xu, J., Wu, Z., Lin, L., & Liu, S. (2014). Selective transformation of 5-hydroxymethylfurfural into the liquid fuel 2,5dimethylfuran over carbon-supported ruthenium. *Industrial and Engineering Chemistry Research*, 53(8), 3056-3064. https://doi.org/10.1021/ie404441a
- IEA. (2024). World Energy Outlook 2024. I. E. Agency. https://www.iea.org/reports/world-energy-outlook-2024
- Insyani, R., Verma, D., Kim, S. M., & Kim, J. (2017). Direct one-pot conversion of monosaccharides into high-yield 2,5-dimethylfuran over a multifunctional Pd/Zr-based metal-organic framework@sulfonated graphene oxide catalyst. *Green Chemistry*, 19(11), 2482-2490. https://doi.org/10.1039/c7gc00269f
- Jha, S., Nanda, S., Acharya, B., & Dalai, A. K. (2022). A Review of Thermochemical Conversion of Waste Biomass to Biofuels. *Energies*, 15(17). https://doi.org/10.3390/en15176352
- Kon Ryu, S., Kyu Lee, W., & Jin Park, S. (2004). Thermal Decomposition of Hydrated Copper Nitrate [Cu(NO 3) 2 ·3H 2 O] on Activated Carbon Fibers. *Carbon letters*, 5 (4), 180-185. https://scispace.com/papers/thermal-decomposition-of-hydrated-copper-nitrate-cu-no-3h-o-89bzrmyvgr
- Lim, H. Y., Rashidi, N. A., Cheah, K. W., & Abdul Manaf, A. S. (2023).

 One Step Microwave Synthesis of 5-Hydroxymethylfurfural from Bamboo in Presence of Low Transition Temperature Mixture.

 Chemical Engineering Transactions, 106, 127-132. https://doi.org/10.3303/CET23106022
- Lim, H. Y., Rashidi, N. A., Othman, M. F. H., Ismail, I. S., Saadon, S. Z. A. H., Chin, B. L. F., Yusup, S., & Rahman, M. N. (2023). Recent advancement in thermochemical conversion of biomass to biofuel. *Biofuels*, *15*(5), 587-604. https://doi.org/10.1080/17597269.2023.2261788
- Ling, P., Hao, Q., Lei, J., & Ju, H. (2015). Porphyrin functionalized porous carbon derived from metal–organic framework as a biomimetic catalyst for electrochemical biosensing. *Journal of Materials Chemistry B*, *3*(7), 1335-1341. https://doi.org/10.1039/C4TB01620C
- Liu, B., & Zhang, Z. (2016). One-Pot Conversion of Carbohydrates into Furan Derivatives via Furfural and 5-Hydroxylmethylfurfural as Intermediates. *ChemSusChem*, *9*(16), 2015-2036. https://doi.org/10.1002/cssc.201600507
- Maiyalagan, T., & Scott, K. (2010). Performance of carbon nanofiber supported Pd–Ni catalysts for electro-oxidation of ethanol in alkaline medium. *Journal of Power Sources*, 195(16), 5246-5251.

- Morales, M., Pielhop, T., Saliba, P., Hungerbühler, K., Rudolf von Rohr, P., & Papadokonstantakis, S. (2017). Sustainability assessment of glucose production technologies from highly recalcitrant softwood including scavengers. *Biofuels, Bioproducts and Biorefining*, 11(3), 441-453. https://doi.org/10.1002/bbb.1756
- Román-Leshkov, Y., Barrett, C. J., Liu, Z. Y., & Dumesic, J. A. (2007).

 Production of dimethylfuran for liquid fuels from biomass-derived carbohydrates. *Nature*, 447(7147), 982-985.

 https://doi.org/10.1038/nature05923
- Saravanan, A., Senthil Kumar, P., Jeevanantham, S., Karishma, S., & Vo, D. V. N. (2022). Recent advances and sustainable development of biofuels production from lignocellulosic biomass. *Bioresource technology*, 344. https://doi.org/10.1016/j.biortech.2021.126203
- Seguel, J., Garcia, R., Chimentao, R. J., Garcia-Fierro, J. L., Ghampson, I. T., Escalona, N., & Sepulveda, C. (2020). Thermal Modification Effect on Supported Cu-Based Activated Carbon Catalyst in Hydrogenolysis of Glycerol. *Materials (Basel)*, 13(3). https://doi.org/10.3390/ma13030603
- Seo, M. W., Lee, S. H., Nam, H., Lee, D., Tokmurzin, D., Wang, S., & Park, Y.-K. (2022). Recent advances of thermochemical conversieon processes for biorefinery. *Bioresource technology*, 343(August 2021), 126109-126109. https://doi.org/10.1016/j.biortech.2021.126109
- Shelepova, E. V., Vedyagin, A. A., Ilina, L. Y., Nizovskii, A. I., & Tsyrulnikov, P. G. (2017). Synthesis of carbon-supported copper catalyst and its catalytic performance in methanol dehydrogenation. Applied Surface Science, 409, 291-295. https://doi.org/10.1016/j.apsusc.2017.02.220
- Son Le, H., Said, Z., Tuan Pham, M., Hieu Le, T., Veza, I., Nhanh Nguyen, V., Deepanraj, B., & Huong Nguyen, L. (2022). Production of HMF and DMF biofuel from carbohydrates through catalytic pathways as a sustainable strategy for the future energy sector. Fuel, 324. https://doi.org/10.1016/j.fuel.2022.124474
- Viar, N., Requies, J. M., Agirre, I., Iriondo, A., García-Sancho, C., & Arias, P. L. (2022). HMF hydrogenolysis over carbon-supported Ni–Cu catalysts to produce hydrogenated biofuels. *Energy*, 255. https://doi.org/10.1016/j.energy.2022.124437
- Wahab, R., Mustafa, M. T., Mohamed, A., Samsi, H. W., & Rasat, M. S. M. (2013). Extractives, Holocellulose, α-Cellulose, Lignin, and Ash Contents in 3 Year-Old Bamboo Culms Gigantochloa Brang, G. Levis, G. Scortechinii and G. Wrayi. Research Journal of Pharmaceutical, Biological and Chemical Sciences, 4(3), 1235-1247. https://www.rjpbcs.com/pdf/2013_4(3)/[132].pdf
- Wang, H., Zhu, C., Li, D., Liu, Q., Tan, J., Wang, C., Cai, C., & Ma, L. (2019). Recent advances in catalytic conversion of biomass to 5-hydroxymethylfurfural and 2, 5-dimethylfuran. *Renewable and Sustainable Energy Reviews*,103, 227-247. https://doi.org/10.1016/j.rser.2018.12.010
- Wang, S., Dai, G., Yang, H., & Luo, Z. (2017). Lignocellulosic biomass pyrolysis mechanism: A state-of-the-art review. *Progress in Energy and Combustion Science*, 62, 33-86. https://doi.org/10.1016/j.pecs.2017.05.004
- Wei, Z., Lou, J., Li, Z., & Liu, Y. (2016). One-pot production of 2,5-dimethylfuran from fructose over Ru/C and a Lewis–Brønsted acid mixture in N,N-dimethylformamide. *Catalysis Science & Technology*, 6(16), 6217-6225. https://doi.org/10.1039/c6cy00275g
- Yadav, V. G., Yadav, G. D., & Patankar, S. C. (2020). The production of fuels and chemicals in the new world: critical analysis of the choice between crude oil and biomass vis-à-vis sustainability and the environment. Clean Technologies and Environmental Policy, 22, 1757-1774. https://doi.org/10.1007/s10098-020-01945-5



© 2025. The Author(s). This article is an open access article distributed under the terms and conditions of the Creative Commons Attribution-ShareAlike 4.0 (CCBY-SA) International License (http://creativecommons.org/licenses/by-sa/4.0/)